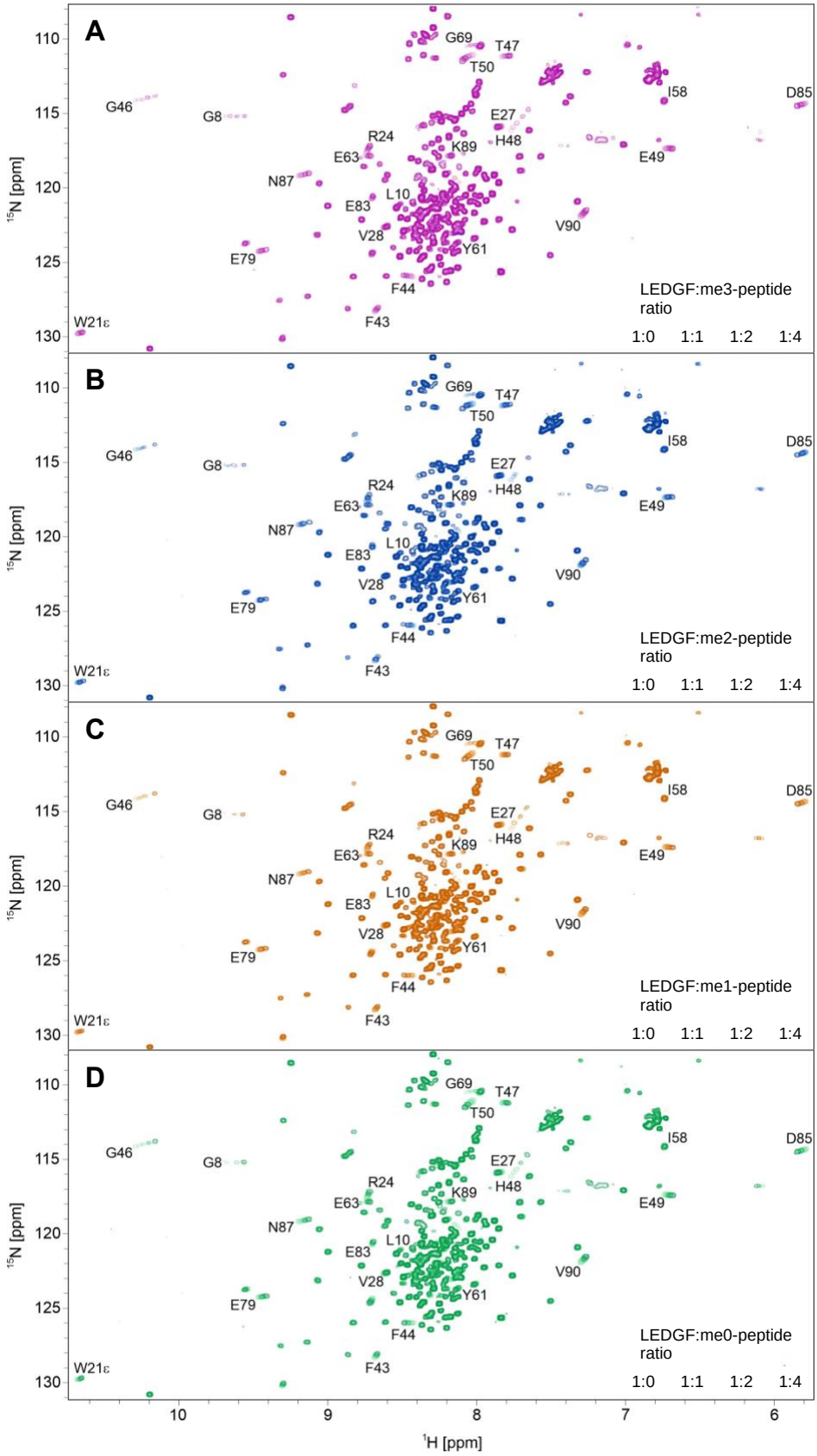

Supplementary figure 1: $^{15}N/^{1}H$ HSQC spectra capturing the chemical shifts upon LEDGF/p52 titration by H3K36me0-3 peptides. (**A**) SAPATGGVK$_{me3}$KPHRY (**B**) SAPATGGVK$_{me2}$KPHRY (**C**) SAPATGGVK$_{me1}$KPHRY (**D**) SAPATGGVKKPHRY

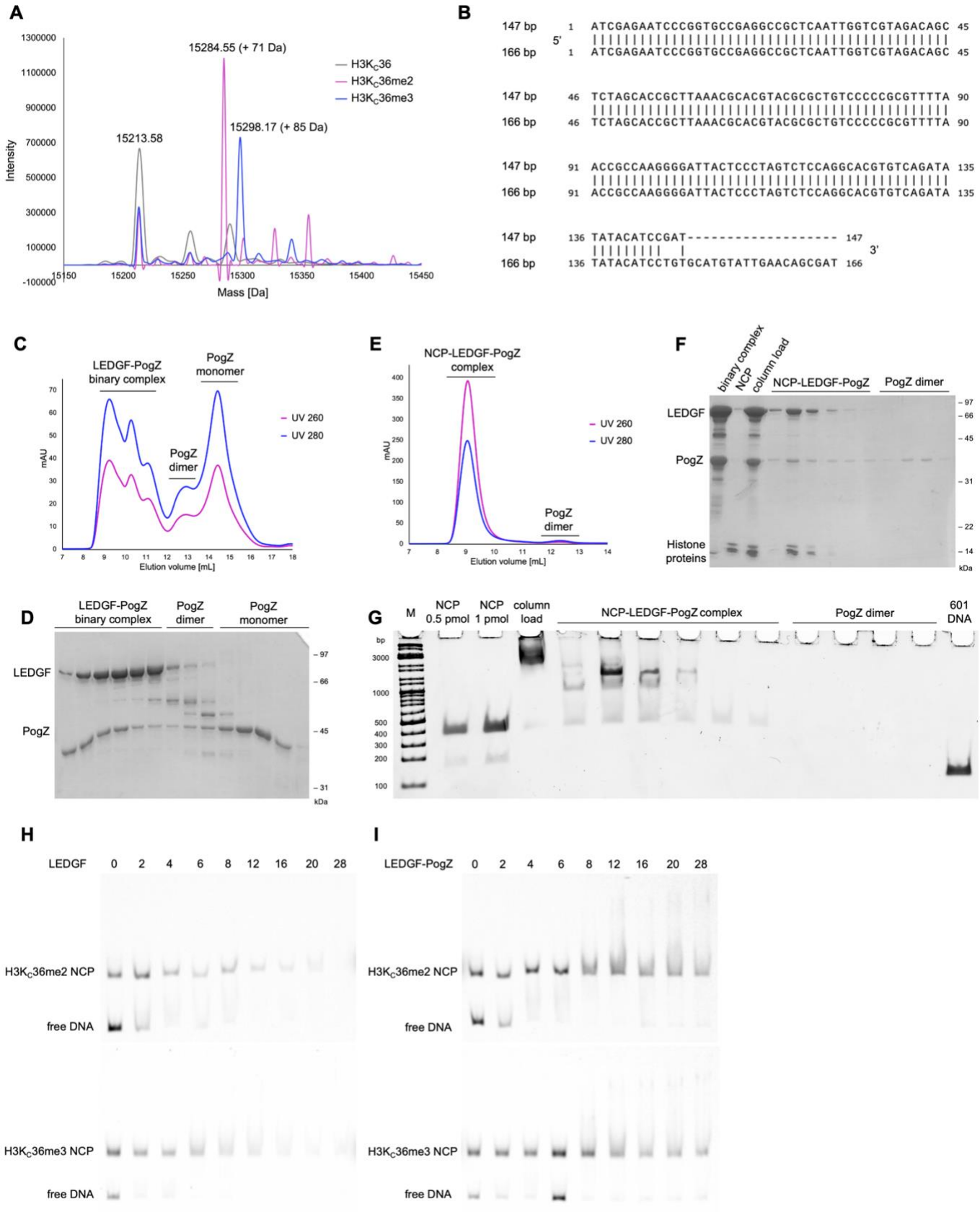
A
15284.55 (+ 71 Da)
15213.58
15298.17 (+ 85 Da)
H3Kc36
H3Kc36me2
H3Kc36me3
Intensity
Mass [Da]
B
147 bp
166 bp
5'
3'
C
LEDGF-PogZ binary complex
PogZ monomer
PogZ dimer
UV 260
UV 280
mAU
Elution volume [mL]
D
LEDGF-PogZ binary complex
PogZ dimer
PogZ monomer
LEDGF
PogZ
kDa
E
NCP-LEDGF-PogZ complex
PogZ dimer
UV 260
UV 280
mAU
Elution volume [mL]
F
binary complex
NCP
column load
NCP-LEDGF-PogZ
PogZ dimer
LEDGF
PogZ
Histone proteins
kDa
G
M
NCP 0.5 pmol
NCP 1 pmol
column load
NCP-LEDGF-PogZ complex
PogZ dimer
601 DNA
bp
H
LEDGF
H3Kc36me2 NCP
free DNA
H3Kc36me3 NCP
free DNA
I
LEDGF-PogZ
H3Kc36me2 NCP
free DNA
H3Kc36me3 NCP
free DNA

Supplementary figure 2: LEDGF/p75-PogZ$_{(1117\text{-}1410)}$ and H3K$_C$36me2/me3 nucleosome complex formation. (**A**) Mass spectrometry data documenting unmodified histone H3K$_C$36 and subsequent H3K$_C$36me2 and H3K$_C$36me3 modifications. (**B**) Canonical 147 bp DNA Widom sequence and its longer 166 bp variant used in nucleosome reconstitution for MST experiments. (**C**) Size-exclusion chromatography elution profile of LEDGF/p75-PogZ$_{(1117\text{-}1410)}$ binary complex. (**D**) SDS-PAGE of accordant fractions collected during SEC, Coomassie Brilliant Blue stained; the gel is distorted due to suboptimal current flow. (**E**) Size-exclusion chromatography elution profile of H3K$_C$36me2 nucleosome complexed with LEDGF/p75-PogZ$_{(1117\text{-}1410)}$. (**F**) SDS-PAGE of accordant fractions collected during SEC, Coomassie Brilliant Blue stained. (**G**) Native PAGE of nucleosomes, 601 Widom DNA and collected SEC fractions, GelRed® stained. (**H**) Representative EMSA of both H3K$_C$36me2 and H3K$_C$36me3 Cy5 labeled 147 bp nucleosomes (indicated as 0) with LEDGF/p75. Molar ratio of LEDGF/p75 to NCP is indicated with numbers. (**I**) Representative EMSA of both H3K$_C$36me2 and H3K$_C$36me3 Cy5 labeled 147 bp nucleosomes (indicated as 0) with LEDGF/p75-PogZ$_{(1117\text{-}1410)}$ binary complex. Molar ratio of LEDGF/p75-PogZ$_{(1117\text{-}1410)}$ binary complex to NCP is indicated with numbers.

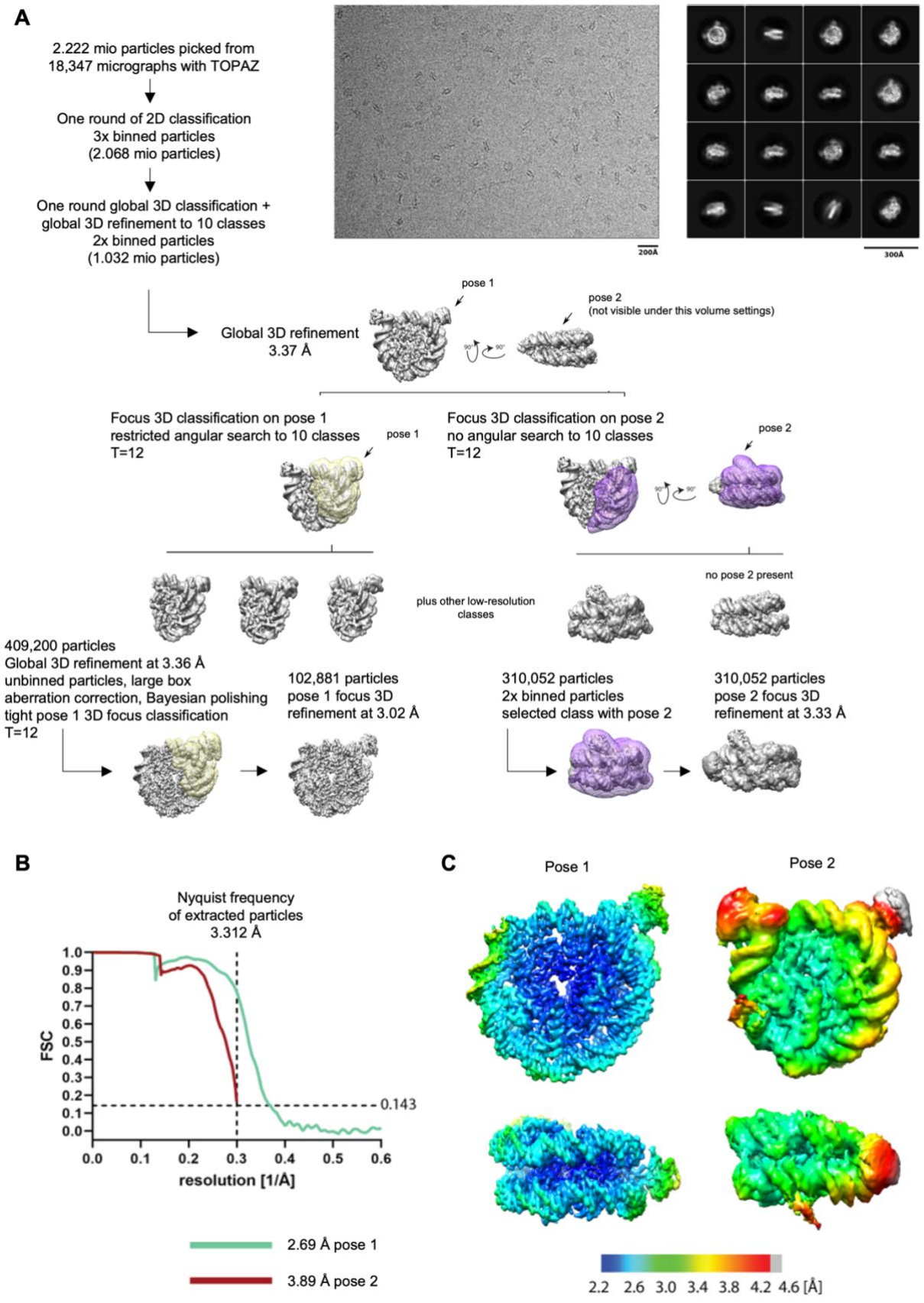
A
2.222 mio particles picked from
18,347 micrographs with TOPAZ
One round of 2D classification
3x binned particles
(2.068 mio particles)
One round global 3D classification +
global 3D refinement to 10 classes
2x binned particles
(1.032 mio particles)
200Å
300Å
Global 3D refinement
3.37 Å
pose 1
pose 2
(not visible under this volume settings)
Focus 3D classification on pose 1
restricted angular search to 10 classes
T=12
Focus 3D classification on pose 2
no angular search to 10 classes
T=12
plus other low-resolution
classes
no pose 2 present
409,200 particles
Global 3D refinement at 3.36 Å
unbinned particles, large box
aberration correction, Bayesian polishing
tight pose 1 3D focus classification
T=12
102,881 particles
pose 1 focus 3D
refinement at 3.02 Å
310,052 particles
2x binned particles
selected class with pose 2
310,052 particles
pose 2 focus 3D
refinement at 3.33 Å
B
Nyquist frequency
of extracted particles
3.312 Å
FSC
resolution [1/Å]
0.143
2.69 Å pose 1
3.89 Å pose 2
C
Pose 1
Pose 2
2.2 2.6 3.0 3.4 3.8 4.2 4.6 [Å]

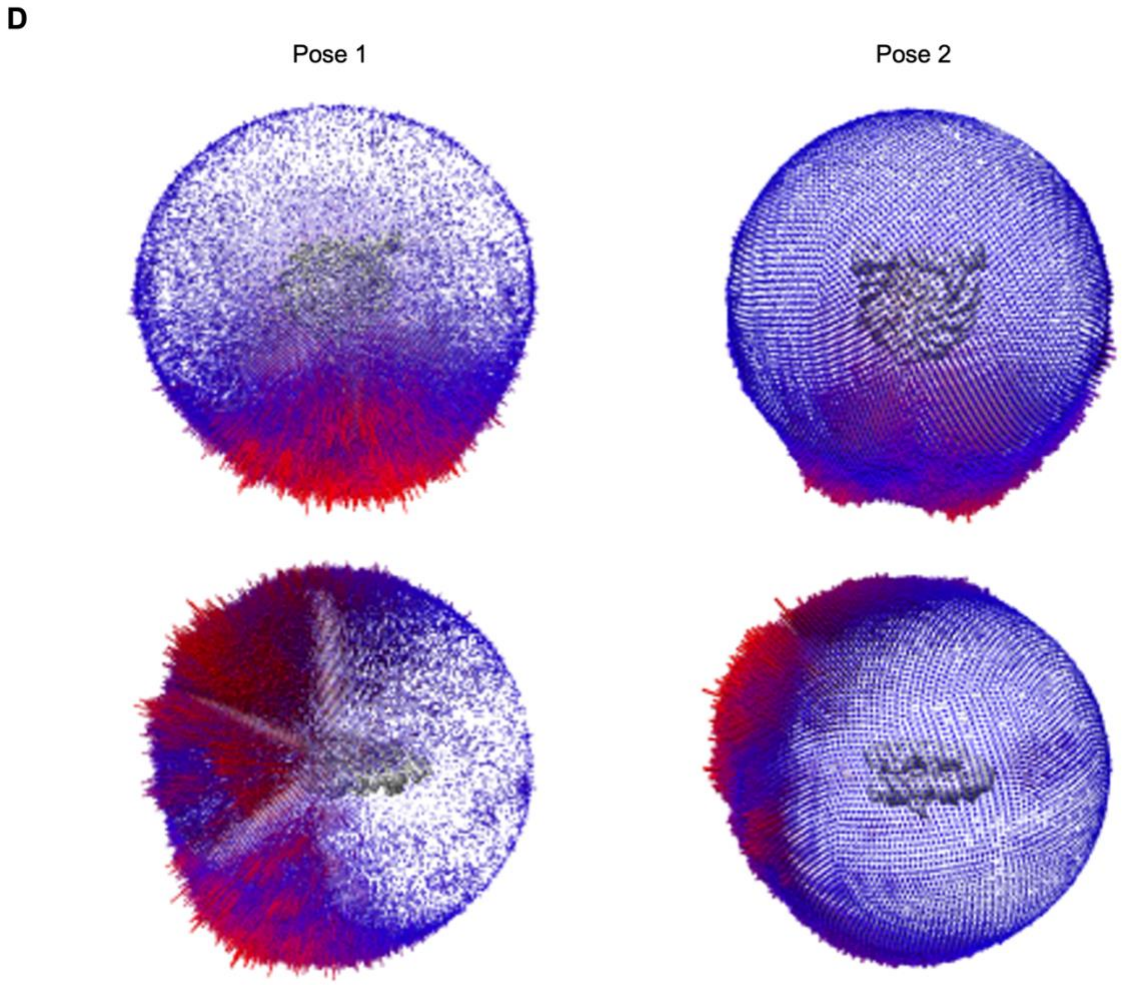

Supplementary figure 3: Cryo-EM data analysis and processing. (**A**) LEDGF/p75-PogZ$_{(1117-1410)}$-H3K$_C$36me2 nucleosome complex data analysis workflow including a representative micrograph in free standing ice, 2D-class averages and 3D classification and refinement scheme. (**B**) Fourier shell correlation (FSC) plot of the two independently refined maps for H3K$_C$36me2 complex in pose 1 (green) and pose 2 (red). The FSC is limited at 3.312 Å resolution which corresponds to the Nyquist frequency of the extracted particles. The overall resolution of the two maps is indicated by the gold standard FSC 0.143 cut-off criteria. (**C**) Surface representation of local resolution distribution of H3K$_C$36me2 complex in pose 1 and pose 2. The map is colored according to the local resolution (as indicated in the color bar) calculated within the RELION software package. (**D**) Angular distribution plots for the final obtained reconstructions of H3K$_C$36me2 complex in pose 1 and pose 2.

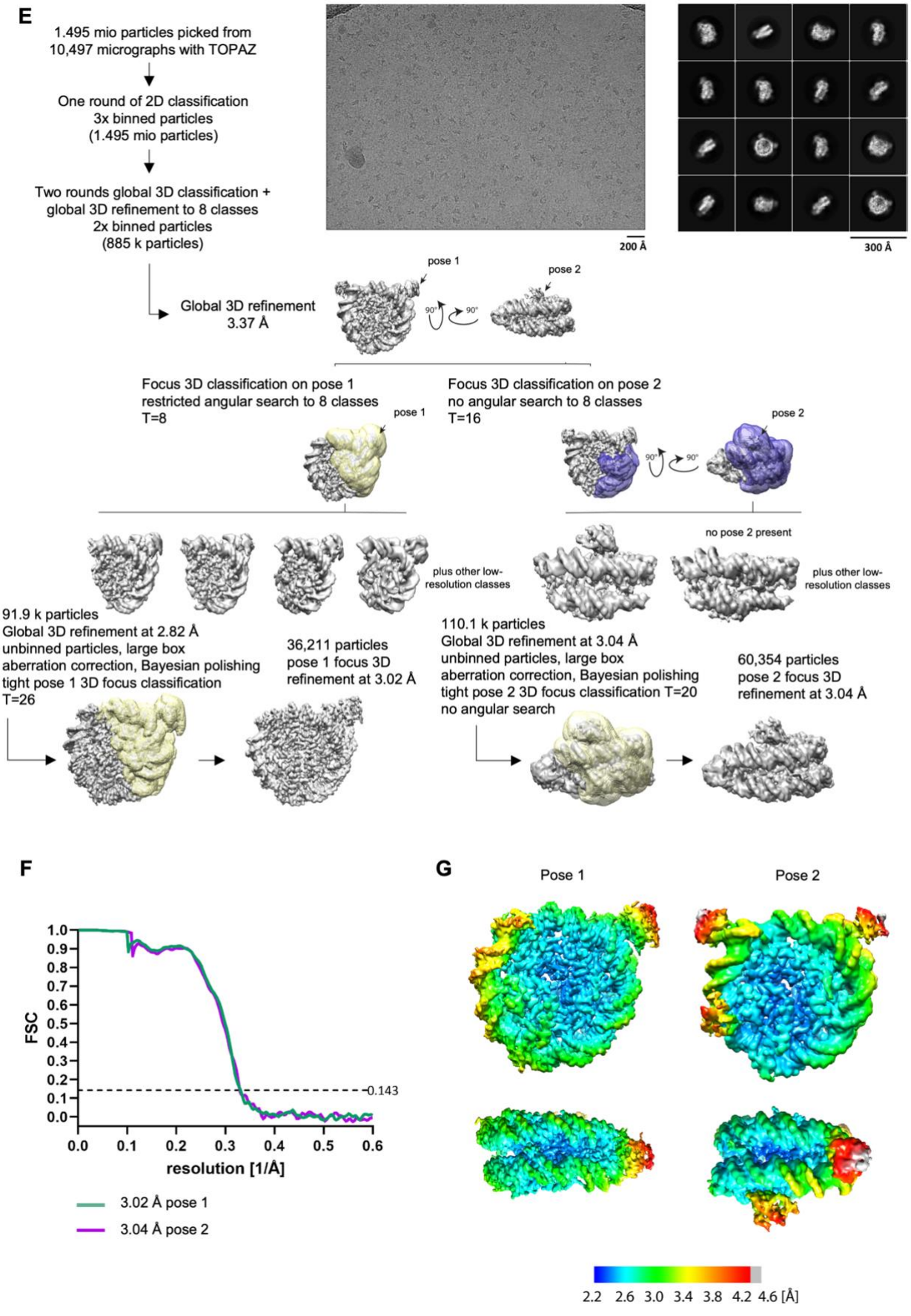
E
1.495 mio particles picked from 10,497 micrographs with TOPAZ
One round of 2D classification 3x binned particles (1.495 mio particles)
Two rounds global 3D classification + global 3D refinement to 8 classes 2x binned particles (885 k particles)
200 Å
300 Å
Global 3D refinement 3.37 Å
pose 1
pose 2
90°
90°
Focus 3D classification on pose 1 restricted angular search to 8 classes T=8
Focus 3D classification on pose 2 no angular search to 8 classes T=16
plus other low-resolution classes
no pose 2 present
plus other low-resolution classes
91.9 k particles Global 3D refinement at 2.82 Å unbinned particles, large box aberration correction, Bayesian polishing tight pose 1 3D focus classification T=26
36,211 particles pose 1 focus 3D refinement at 3.02 Å
110.1 k particles Global 3D refinement at 3.04 Å unbinned particles, large box aberration correction, Bayesian polishing tight pose 2 3D focus classification T=20 no angular search
60,354 particles pose 2 focus 3D refinement at 3.04 Å
F
FSC
1.0
0.9
0.8
0.7
0.6
0.5
0.4
0.3
0.2
0.1
0.0
0.143
0.0 0.1 0.2 0.3 0.4 0.5 0.6
resolution [1/Å]
3.02 Å pose 1
3.04 Å pose 2
G
Pose 1
Pose 2
2.2 2.6 3.0 3.4 3.8 4.2 4.6 [Å]

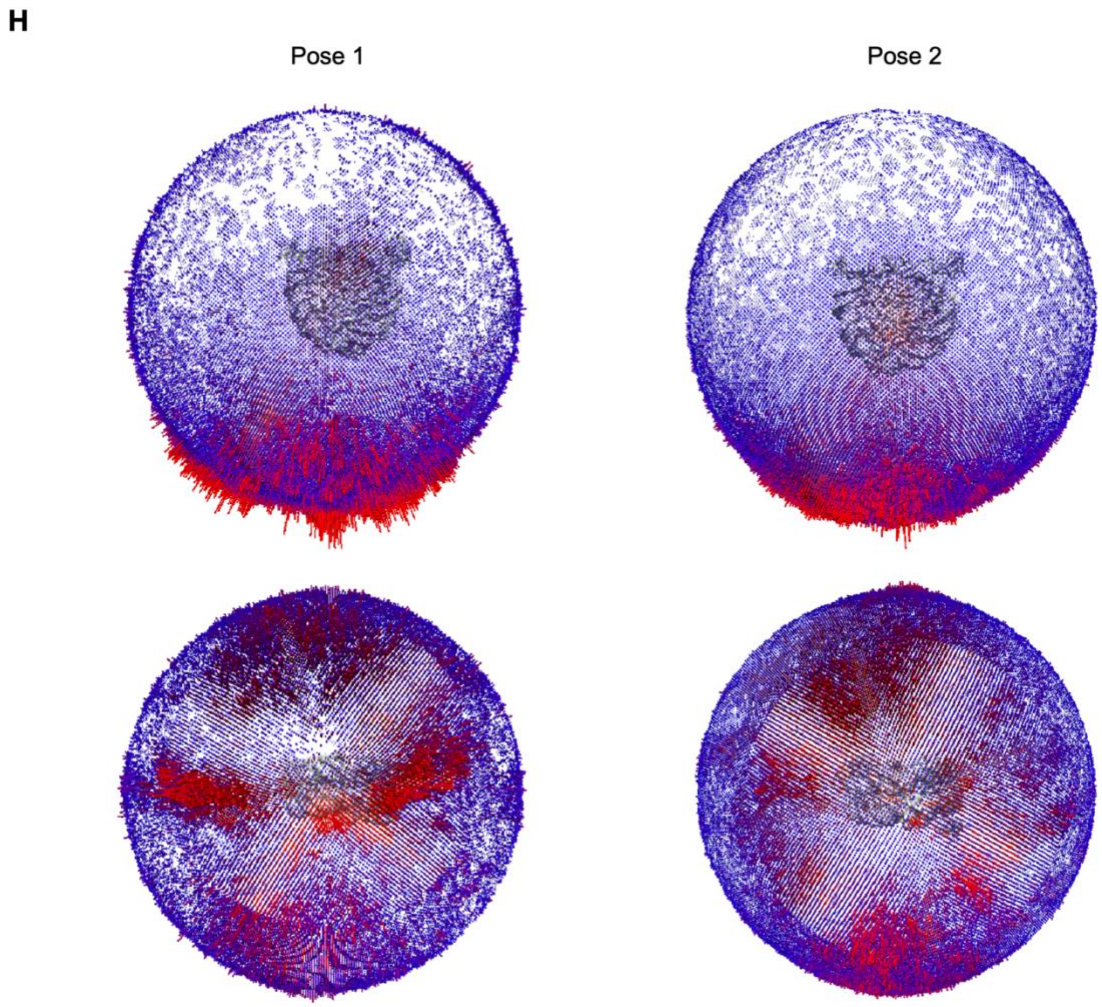

Supplementary figure 3: Cryo-EM data analysis and processing. (**E**) LEDGF/p75-PogZ$_{(1117-1410)}$-H3K$_C$36me3 nucleosome complex data analysis workflow including a representative micrograph in free standing ice, 2D-class averages and 3D classification and refinement scheme. (**F**) Fourier shell correlation (FSC) plot of the two independently refined maps for H3K$_C$36me3 complex in pose 1 (teal) and pose 2 (magenta). The overall resolution of the two maps is indicated by the gold standard FSC 0.143 cut-off criteria. (**G**) Surface representation of local resolution distribution of H3K$_C$36me3 complex in pose 1 and pose 2. The map is colored according to the local resolution (as indicated in the color bar) calculated within the RELION software package. (**H**) Angular distribution plots for the final obtained reconstructions of H3K$_C$36me3 complex in pose 1 and pose 2.

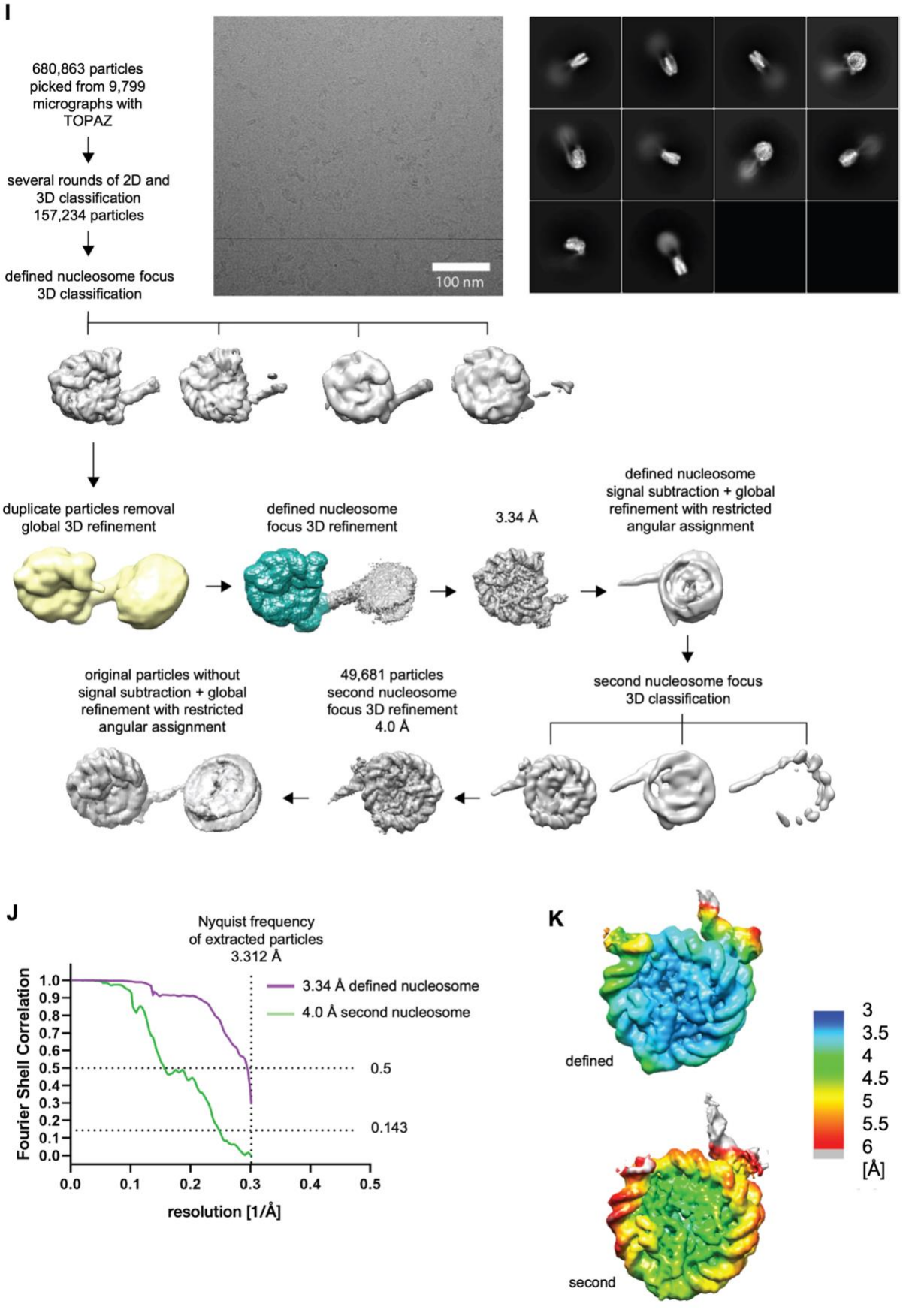
I
680,863 particles picked from 9,799 micrographs with TOPAZ
several rounds of 2D and 3D classification 157,234 particles
defined nucleosome focus 3D classification
100 nm
duplicate particles removal global 3D refinement
defined nucleosome focus 3D refinement
3.34 Å
defined nucleosome signal subtraction + global refinement with restricted angular assignment
second nucleosome focus 3D classification
49,681 particles second nucleosome focus 3D refinement 4.0 Å
original particles without signal subtraction + global refinement with restricted angular assignment
J
Nyquist frequency of extracted particles 3.312 Å
3.34 Å defined nucleosome
4.0 Å second nucleosome
0.5
0.143
Fourier Shell Correlation
resolution [1/Å]
K
defined
second
3
3.5
4
4.5
5
5.5
6
[Å]

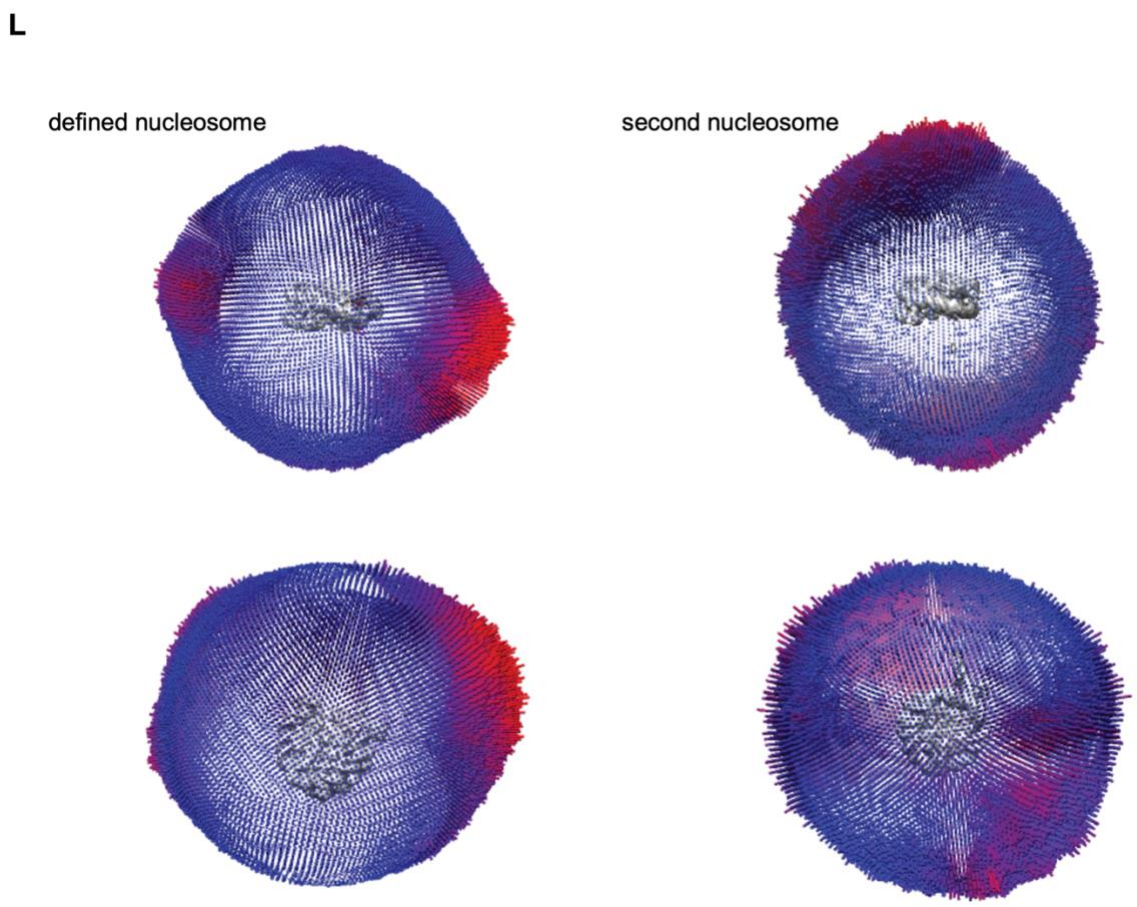

Supplementary figure 3: Cryo-EM data analysis and processing. (**I**) Data analysis workflow including a representative micrograph of LEDGF/p75-PogZ$_{(1117\text{-}1410)}$-H3K$_C$36me3 dinucleosome complex in free standing ice after MotionCor2 correction at defocus of ~2.5 µm, 2D-class averages, and 3D classification and refinement scheme. (**J**) FSC plot of the two independently refined maps for defined nucleosome (green) and for second nucleosome (purple). The FSC is limited at 3.34 Å resolution which corresponds to the Nyquist frequency of the extracted particles. (**K**) Surface representation of local resolution distribution of the defined and for second nucleosome. The map is colored according to the local resolution (as indicated in the color bar) calculated within the RELION software package. (**L**) Angular distribution plots for the final obtained reconstructions for defined and second nucleosome.

A

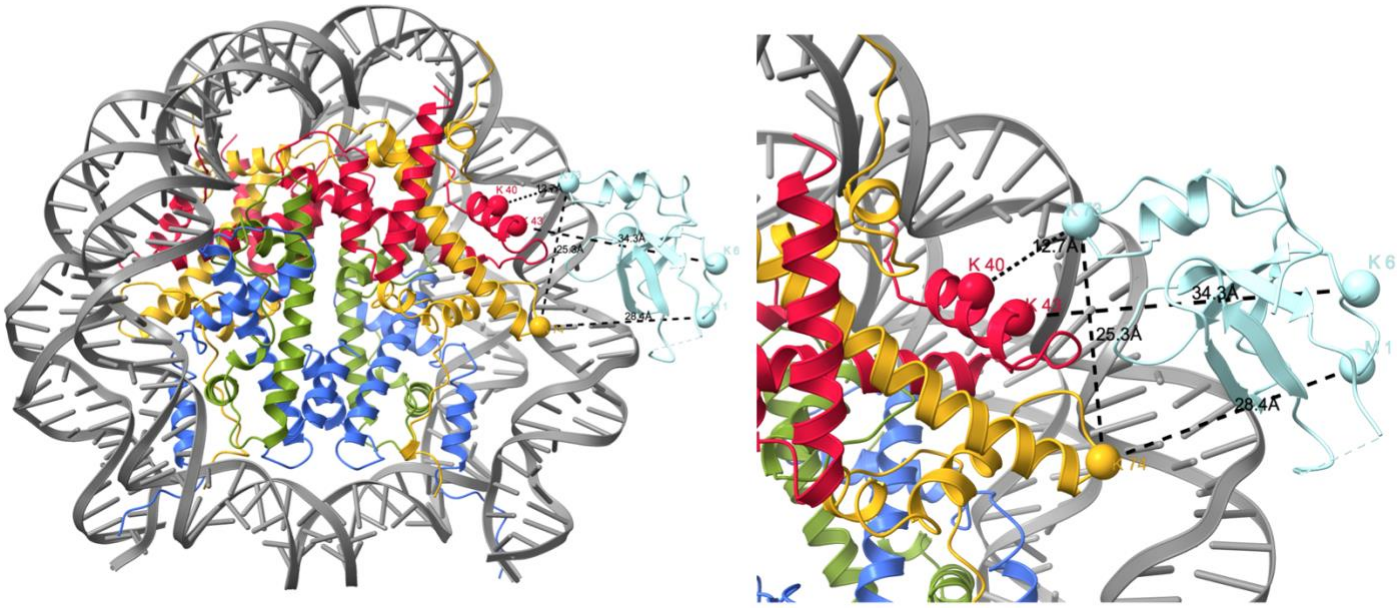

B

Protein1	Protein2	AbsPos1	Residue	AbsPos2	Residue	Distance in model
>sp|P06897|H2A_Xenopus	>sp|O75475|LEDGF_Human	74	K	1	M	28.4
>sp|P06897|H2A_Xenopus	>sp|O75475|LEDGF_Human	74	K	73	K	25.3
>sp|P02281|H2B_Xenopus	>sp|O75475|LEDGF_Human	40	K	73	K	12.7
>sp|P02281|H2B_Xenopus	>sp|O75475|LEDGF_Human	43	K	6	K	34.3
>sp|P06897|H2A_Xenopus	>sp|O75475|LEDGF_Human	74	K	251	K	--

Supplementary figure 4: Crosslinks identified between the nucleosome and LEDGF/p75 in its alternative pose. (**A**) View of the whole nucleosome with PWWP domain (pale blue) in alternative pose and a close-up of this region. Protein chains are represented as cartoons, whereas Cα of crosslinked amino acids are shown as balls. These specific residues and observed distances between Cα are indicated. (**B**) Table summarizes all the observed crosslinks between the nucleosome and LEDGF/p75.

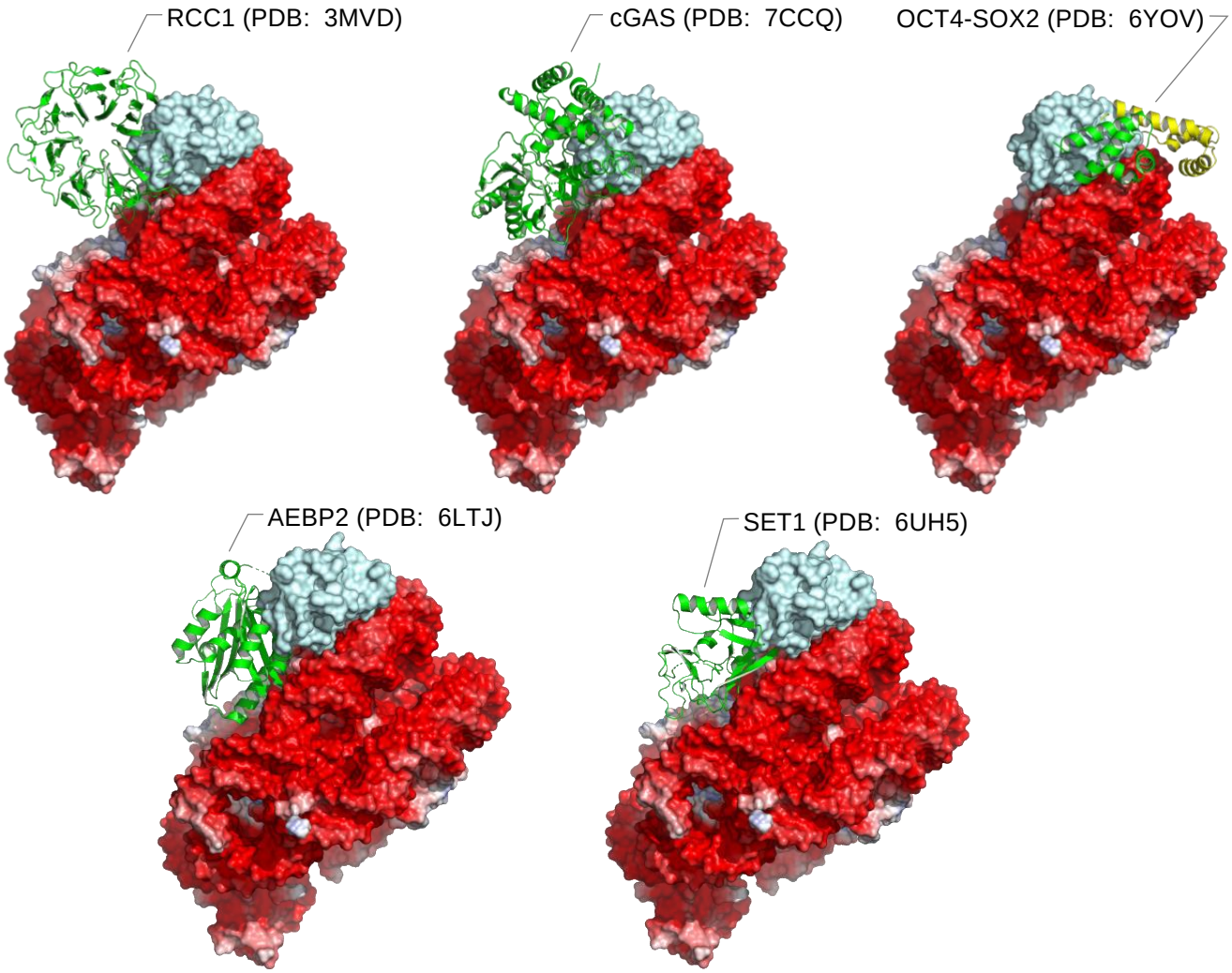

Supplementary figure 5: Minimal overlap between the non-canonical PWWP pose and other nucleosome interacting proteins. NPC is show in surface representation with color-coded charge distribution. The PWWP domain pose 2 is in cyan and the other NPC-interaction domains in green.

A

5' Cy5-C T G G A G A A T C C C G G T G C C G A G 3'

5' C T G G A G A A T C C C G G T G C C G A G G C C G C T C A A T T G G T C G T A G A C A G C T C T A G C
A C C G C T T A A A C G C A C G T A C G C G C T G T C C C C C G C G T T T T A A C C G C C A A G G G G A
T T A C T C C C T A G T C T C C A G G C A C G T G T C A G A T A T A T A C A T C C T G T 3'

B

5' A T C G A G A A T C C C G G T G C C G A G G C C G C T C A A T T G G T C G T A G A C A G C T C T A G C
A C C G C T T A A A C G C A C G T A C G C G C T G T C C C C C G C G T T T T A A C C G C C A A G G G G A
T T A C T C C C T A G T C T C C A G G C A C G T G T C A G A T A T A T A C A T C C G A T 3'

5' A T C G A G A A T C C C G G T G C C G A G G C C G C T C A A T T G G T C G T A G A C A G C T C T A G C
A C C G C T T A A A C G C A C G T A C G C G C T G T C C C C C G C G T T T T A A C C G C C A A G G G G A
T T A C T C C C T A G T C T C C A G G C A C G T G T C A G A T A T A T A C A T C C T G T G C A T G T A T T
G A A C A G C G A T 3'

C

5' A T C G A G A A T C C C G G T G C C G A G G C C G C T C A A T T G G T C G T A G A C A G C T C T A G C
A C C G C T T A A A C G C A C G T A C G C G C T G T C C C C C G C G T T T T A A C C G C C A A G G G G A
T T A C T C C C T A G T C T C C A G G C A C G T G T C A G A T A T A T A C A T C C G A T G C A T G T A A G
T A C T G G C C G C C A T C G A G A A T C C C G G T G C C G A G G C C G C T C A A T T G G T C G T A G A
C A G C T C T A G C A C C G C T T A A A C G C A C G T A C G C G C T G T C C C C C G C G T T T T A A C C
G C C A A G G G G A T T A C T C C C T A G T C T C C A G G C A C G T G T C A G A T A T A T A C A T C C G A
T 3'

D

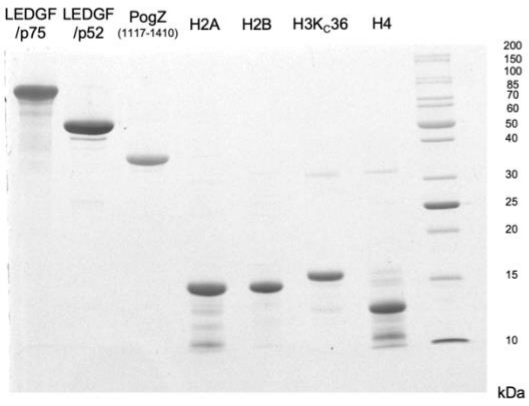

Supplementary figure 6: DNA sequences used for nucleosome and dinucleosome reconstitution and proteins used in this study. (**A**) The 5' Cy5-labeled primer and a respective 5' Cy5-labeled PCR-produced Widom 601 147 bp dsDNA used for EMSA. (**B**) Widom 601 147 bp and 166 bp dsDNA produced via restriction digest of high copy number plasmid and used for cryo-EM, MST, NMR and XL-MS experiments. This sequence variant is only different by containing half of EcoRV cleavage site at the beginning and the end, so it can be efficiently liberated from the plasmid. The production method was changed during the experimental process due to higher yield demand. (**C**) Widom 601-based 314 bp dsDNA produced via restriction digest of high copy number plasmid and used for dinucleosome reconstitution. The 20 bp linker sequence between the two Widom 601 sequences is underlined. (**D**) SDS-PAGE of individual proteins used in this study, Coomassie Brilliant Blue stained.

Name of structure	**H3K$_C$36 me2 pose1**	**H3K$_C$36 me2 pose2**	**H3K$_C$36 me3 pose1**	**H3K$_C$36 me3 pose2**	**H3K$_C$36 dinuc. defined**	**H3K$_C$36 dinuc. second**
PDB ID	8PEO	8PEP	8PC5	8PC6	8CBN*	8CBQ*
EMDB ID	EMD-17633	EMD-17634	EMD-17594	EMD-17595	EMD-16546	EMD-16549
Data collection and processing						
Microscope	FEI Titan Krios		FEI Titan Krios		FEI Titan Krios	
Voltage (kV)	300		300		300	
Camera	Gatan K3 BioQuantum		Gatan K3 BioQuantum		Gatan K2	
Magnification	165,000x		165,000x		165,000x	
Nominal defocus range (μm)	1.2-3.1		0.9-3.0		1.2-3.2	
Exposure time (s)	2s		2s		8s	
Electron exposure (e–/Å^2)	40		42		55	
Number of frames collected (no.)	40		40		40	
Number of frames processed (no.)	22		22		40	
Pixel size (Å)	0.8336		0.8336		0.822	
Micrographs (no.)	18,347		10,497		9,799	
Total particle images (no.)	2,222,076		1,495,263		680,863	
Refinement						
Particles per class (no.)	102881	310052	36,211	60,354	154,229	49,681
Map resolution (Å), 0.143 FSC	2.69	3.33	3.02	3.04	3.34	4.0
Model resolution (Å), 0.5 FSC	2.9	3.4	3.1	3.2	NA	NA
Map sharpening *B* factor (Å^2)	-40.28	-67.66	-59.44	-64.37	-80.53	-143.77
Map versus model cross-correlation (CCmask)	0.86	0.87	0.84	0.84	NA	NA
Model composition						
Non-hydrogen atoms	12,835	13,492	12,836	13,493	NA	NA
Protein residues	852	938	853	939	NA	NA
Nucleotide residues	294	294	294	294	NA	NA
Water	0	0	0	0	NA	NA
Ligands	1	1	0	0	NA	NA
***B* factors (Å^2)**						
Protein	44.93	115.62	32.44	38.44	NA	NA
Nucleotide	83.41	115.71	83.71	79.58	NA	NA
Ligand	81.46	189.75	NA	NA	NA	NA
Water	NA	NA	NA	NA	NA	NA
R.M.S. deviations						
Bond lengths (Å)	0.005	0.004	0.006	0.004	NA	NA
Bond angles (°)	0.768	0.712	0.779	0.677	NA	NA
Validation						
MolProbity score	1.44	1.50	1.40	1.47	NA	NA
All-atom clashscore	8.08	9.42	7.30	7.87	NA	NA
Poor rotamers (%)	0.14	0.13	0.42	0.13	NA	NA
Ramachandran plot						
Favored (%)	98.07	98.14	98.07	97.81	NA	NA
Allowed (%)	1.93	1.86	1.93	2.19	NA	NA
Outliers (%)	0	0	0	0	NA	NA

Supplementary table 1: CryoEM structure determination and validation statistics. *PDB model 6S01 was used for rigid body docking into the EMD-16546 and EMD-16549 cryo-EM maps.